The interaction of circulating cells with tumors: pharmacokinetic and fluid dynamic models

Lance L. Munn
Steele Lab for Tumor Biology

Outline

- Clinical study of anti-angiogenic therapy
- Pharmacokinetic model of angiogenesis and tumor growth: contribution of endothelial precursor cells
- Fluid dynamics of cell trafficking

Clinical data

- Phase 1 clinical trial treating patients with rectal cancer
- Day 0: Anti-VEGF antibody (bevacizumab) 5mg/kg
- Day 3: blood sample-circulating EPCs
- Day 12: sigmoidoscopy, biopsy, functional CT, PET
- Day 14: 5 fluorouracil + radiation
- Day 100: surgery

Anti-VEGF treatment decreases vascular density

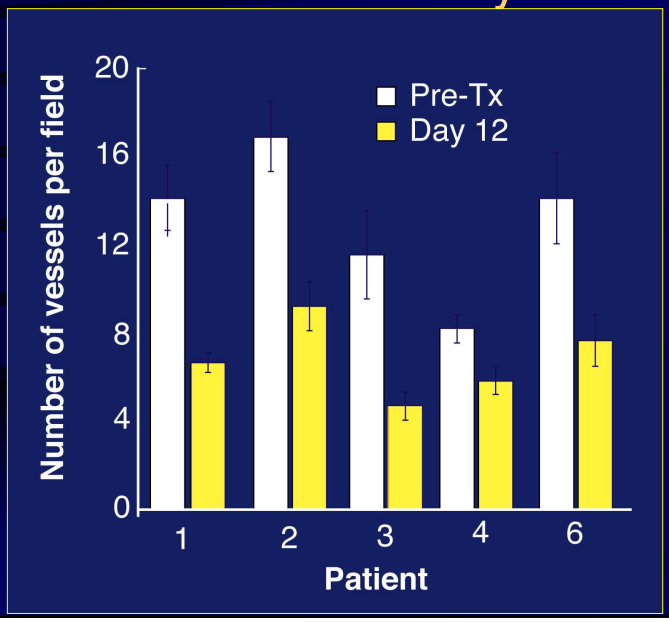

Anti-VEGF treatment decreases blood flow and blood volume

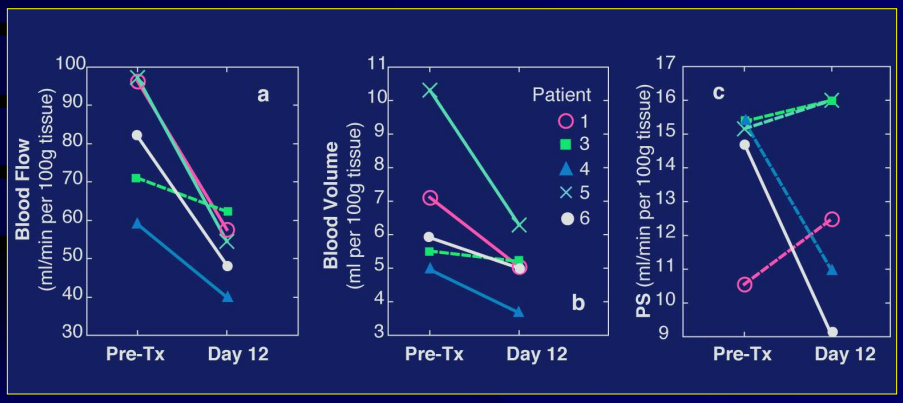

Tumor regression in response to anti-VEGF

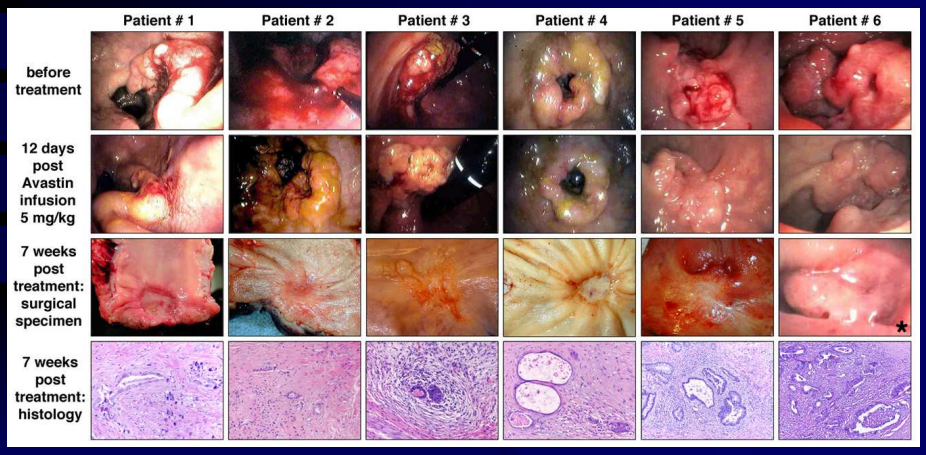

Circulating endothelial cells decrease after anti-VEGF

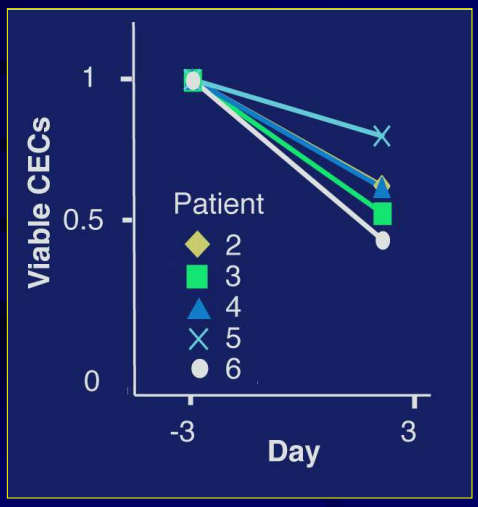

Clinical data

- Phase 1 clinical trial treating patients with rectal cancer
- Day 0: Anti-VEGF antibody (bevacizumab) 5mg/kg
- Day 3: blood sample-circulating EPCs
- Day 12: sigmoidoscopy, biopsy, functional CT, PET
- Day 14: 5 fluorouracil + radiation
- Day 100: surgery

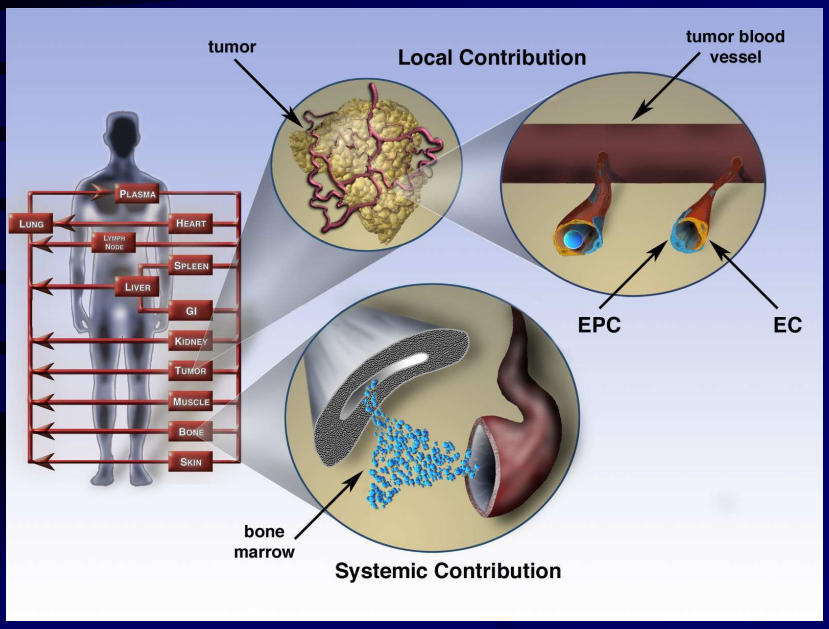

Goal

Quantify the relative contributions of endothelial and endothelial progenitor cells to angiogenesis.

Local and systemic contributions to angiogenesis are described by a tumor growth and angiogenesis model and a physiologically-based cell biodistribution model, respectively

Background

- **Tumors are dependent upon neovascularization to emerge from dormancy and grow; angiogenic phenotype is dependent on balance between stimulators and inhibitors**
  (Hanahan and Folkman, 1996; Holmgren, *et al.* 1995)
- **Certain primary tumors are able to suppress the growth of metastases through production of angiogenesis inhibitors**
  (O'Reilly *et al.* 1994)
- **Tumors frequently exhibit regions of necrosis amidst neovascularization in regions where blood flow is inadequate**
  (Endrich *et al.* 1979)

Primary tumor affects secondary growth

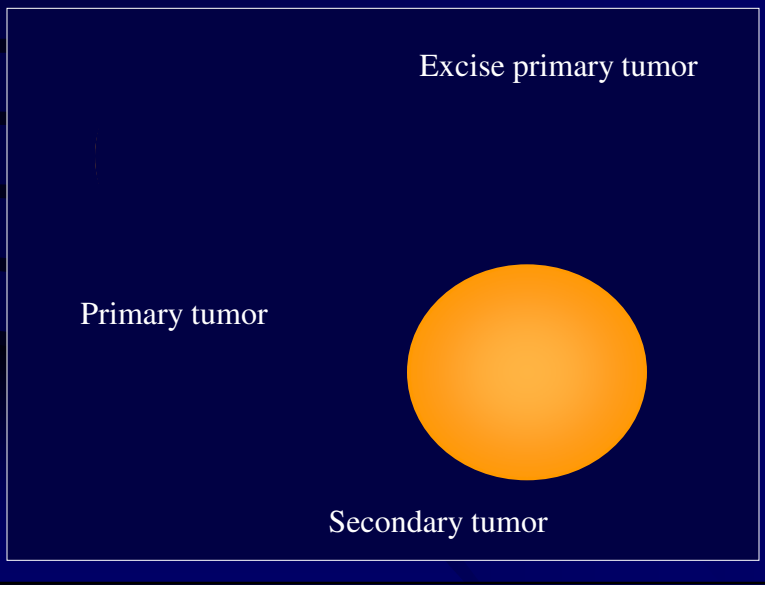

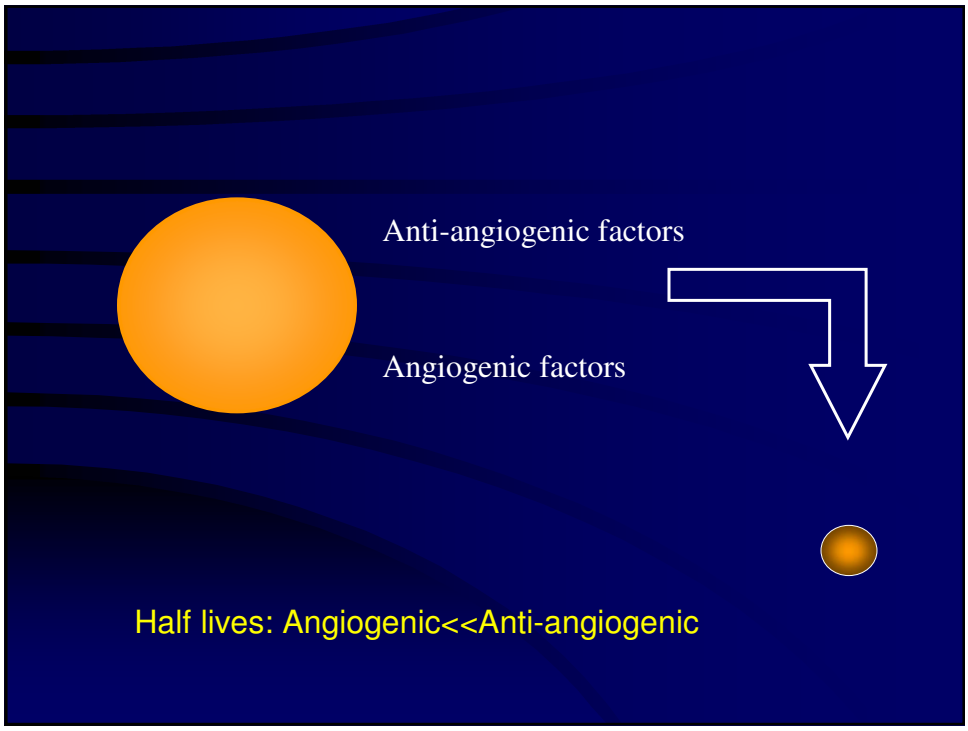

Model Equations

Governing equation:

$$D_{i/j}^{+/-}\nabla_r^2 C_{i/j}^{+/-} + g_{i/j}^{+/-} - k_{i/j}^{+/-} C_{i/j}^{+/-} = 0$$

Boundary conditions:

$$C_i^{+/-}\Big|_{r=R_t} = C_j^{+/-}\Big|_{r=R_t}$$

$$D_i^{+/-}\frac{dC_i^{+/-}}{dr}\Big|_{r=R_t} = D_j^{+/-}\frac{dC_j^{+/-}}{dr}\Big|_{r=R_t}$$

$$\frac{dC_i^{+/-}}{dr}\Big|_{r=0} = 0$$

$$\frac{dC_j^{+/-}}{dr}\Big|_{r=\infty} = 0$$

Assumptions, constraints:

$$D_i^{+/-} \sim D_j^{+/-}$$

$$D_{i/j}^{+} \geq D_{i/j}^{-}$$

$$\gamma_i^{+/-}, \Gamma_i^{+/-} \geq \gamma_j^{+/-}, \Gamma_j^{+/-}$$

$$\gamma_i^{+/-} \geq \Gamma_i^{+/-}$$

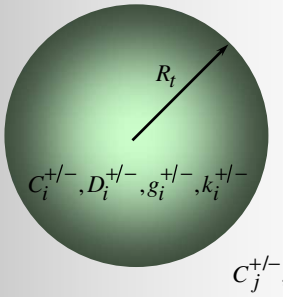

$C_j^{+/-}, D_j^{+/-}, g_j^{+/-}, k_j^{+/-}$

Angiogenic activity varies within the tumor

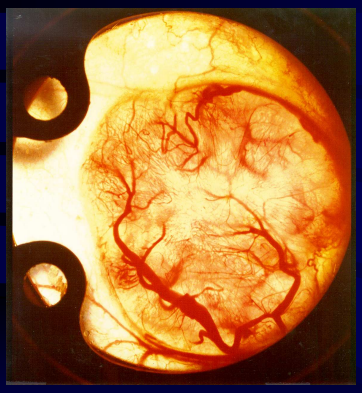

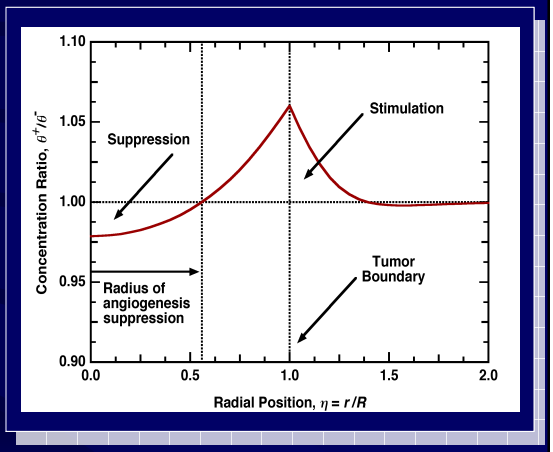

Angiogenic activity varies with tumor size

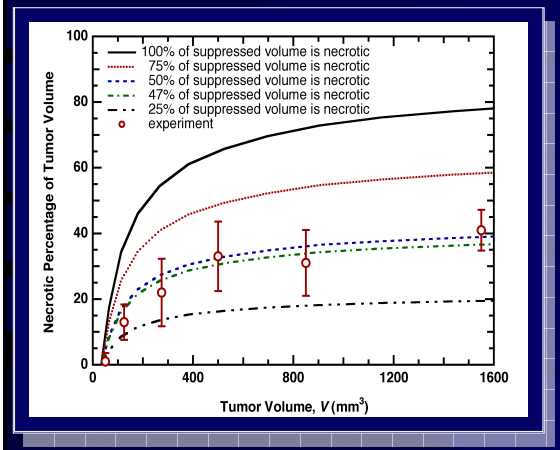

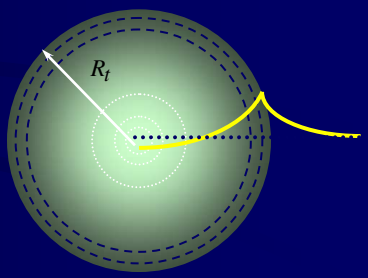

Increasing distance from primary results in more inhibition

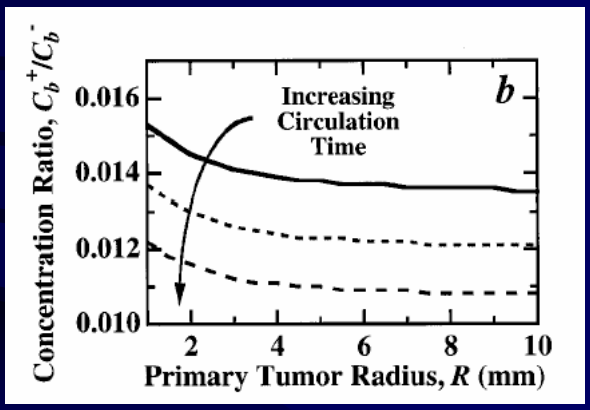

Ramanujan et al., Cancer Research, 2000

Summary

- The formation of central necrosis may be mediated by the imbalance between angiogenesis stimulators and inhibitors
- Highest angiogenesis stimulation occurs near the tumor periphery and in the peri-tumor normal tissue consistent with observations

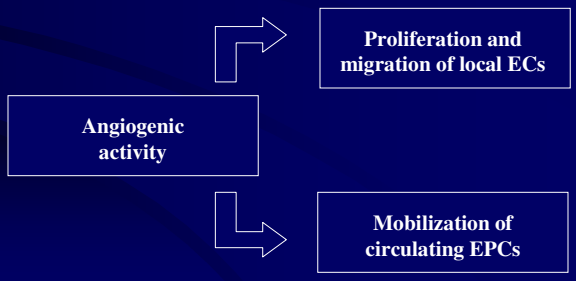

SCHEMATIC OF PHYSIOLOGICALLY-BASED PHARMACOKINETIC MODEL

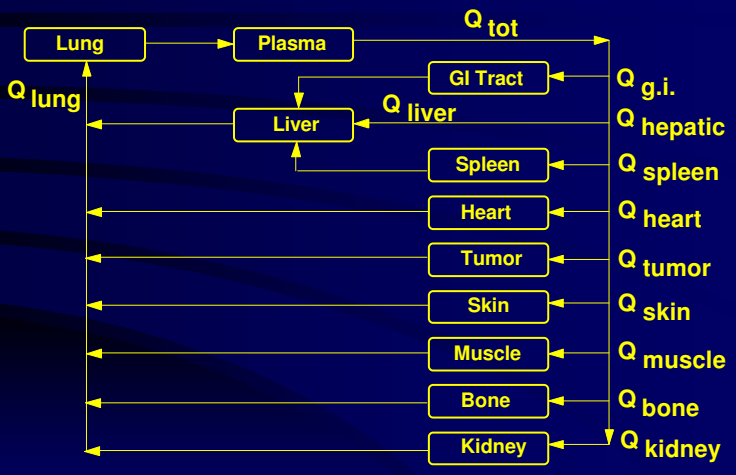

Angiogenic tendency

$$\alpha = \begin{cases} \frac{\theta^+}{\theta^-} - 1 & \alpha \geq 0 \\ 1 - \frac{\theta^-}{\theta^+} & \alpha < 0 \end{cases}$$

Tumor growth

$$\frac{dR_t}{dt} = \frac{1}{R_t^2} \int_0^{R_t} g(r) r^2 dr$$

Compartment fluxes

$$\frac{d\left(V_{v,i} C_i^j\right)}{dt} = Q_i \left(C_{i,in}^j - C_{i,out}^j\right) + G_i^j - k_i^j C_{i,out}^j$$

EPC incorporation

$$\frac{d\rho_v^{EPC}}{dt} = k_2 \rho_v^{EPC} \left(k_3 - \rho_v^{EPC}\right) + \begin{cases} k_4 \rho_v^{EC} \alpha q^{EPC} & \alpha > 0 \\ 0 & \alpha \leq 0 \end{cases}$$

Angiogenic activity is highest at tumor periphery

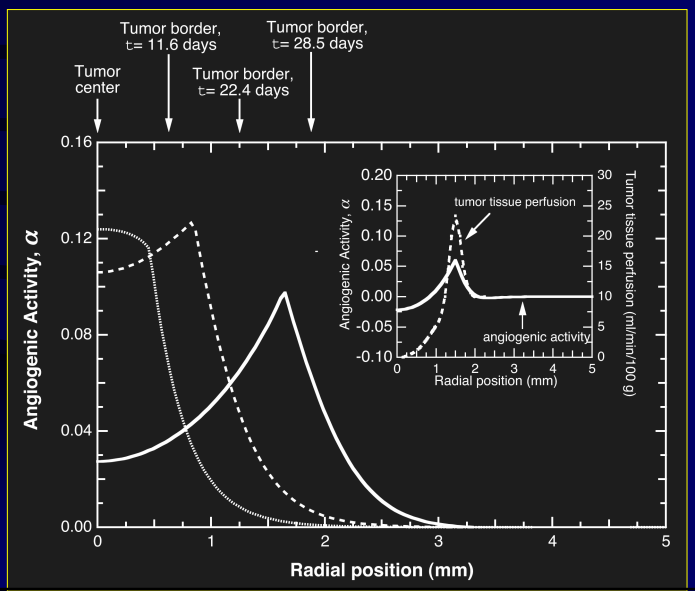

Vascular density reflects angiogenic activity

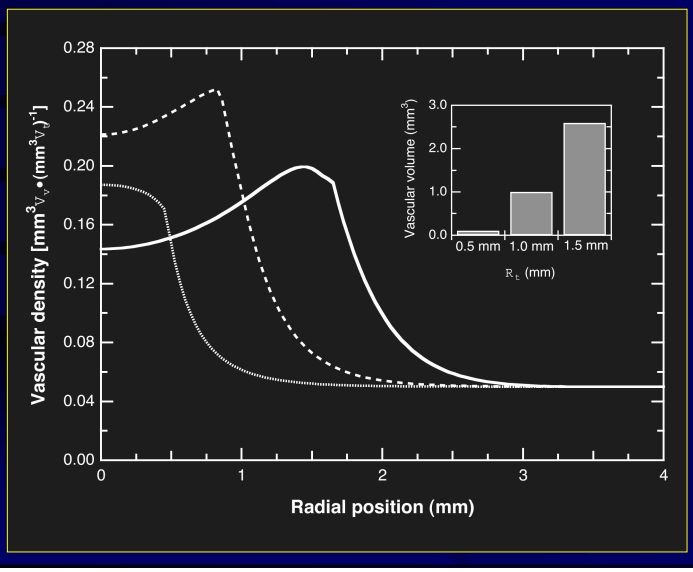

EPC contribution is small…

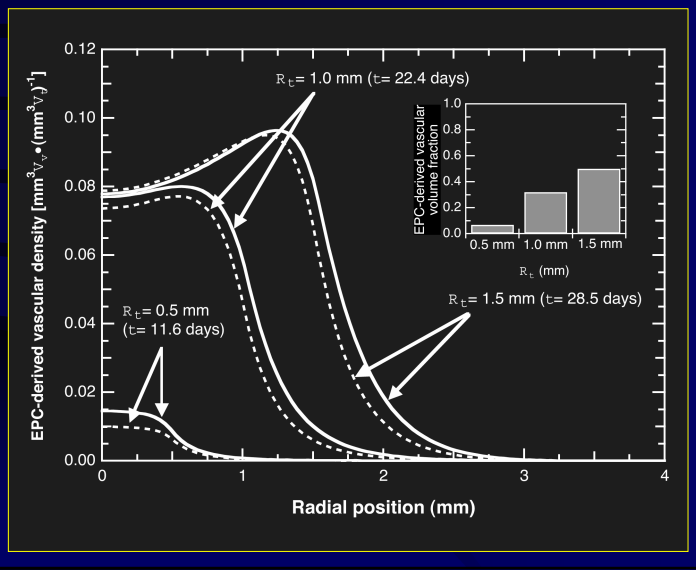

…but significantly affects growth

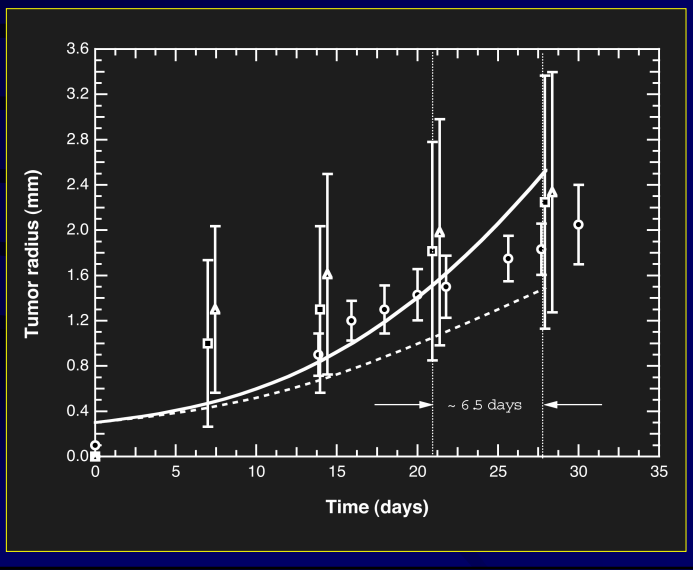

Anti-VEGF treatment affects systemic and local angiogenic pathways

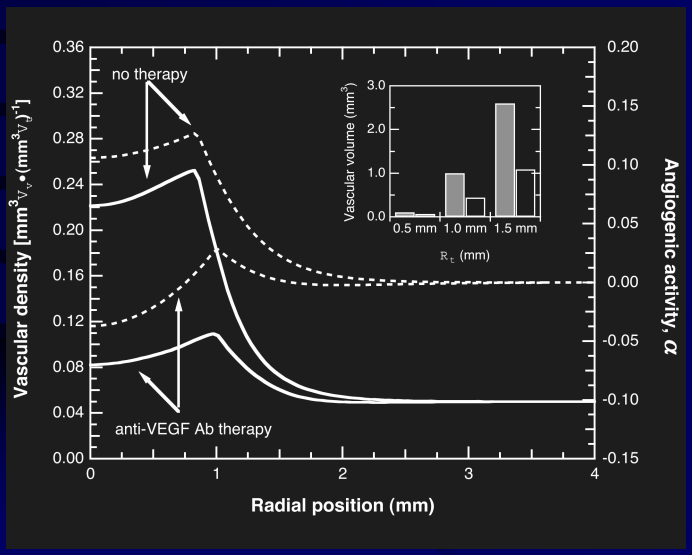

Growth delay predictions for various therapies

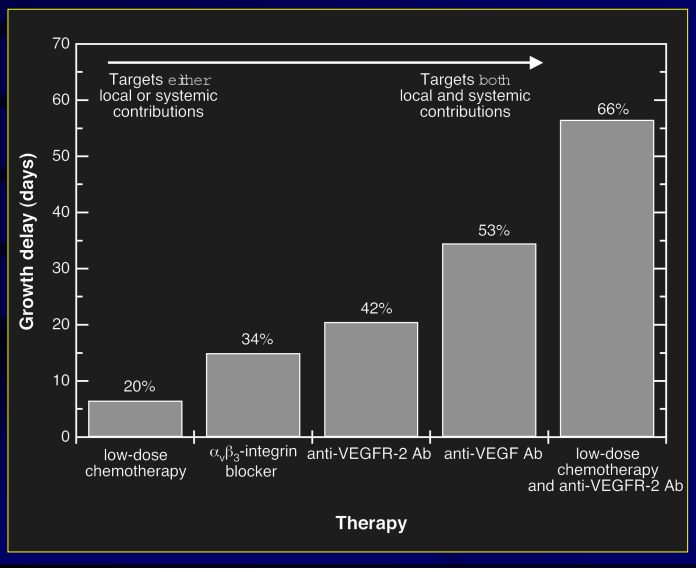

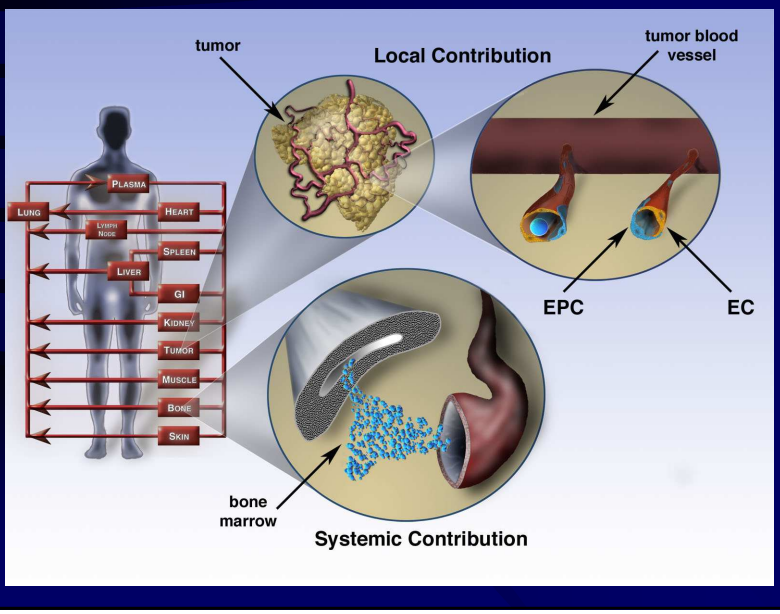

Blood fluid dynamics and leukocyte adhesion

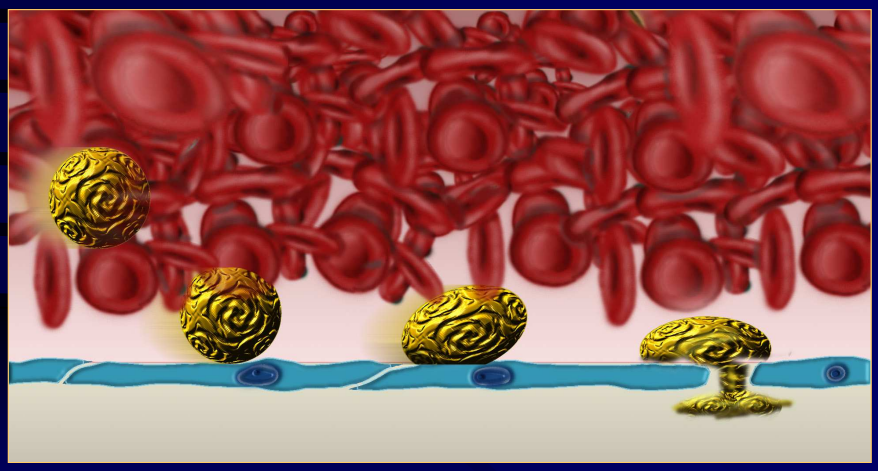

RBCs enhance leukocyte-endothelium interactions

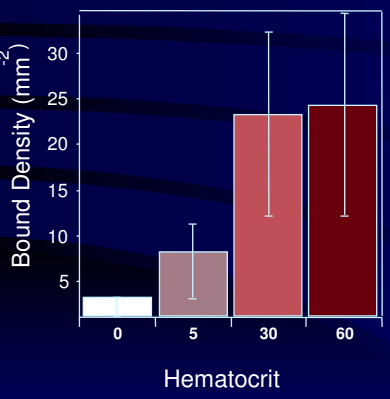

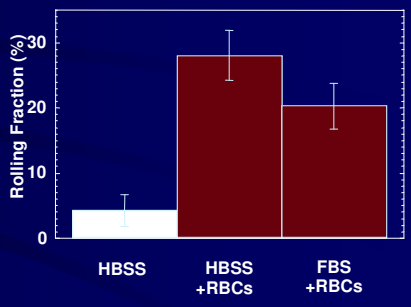

Permissive shear stress range is extended with RBCs

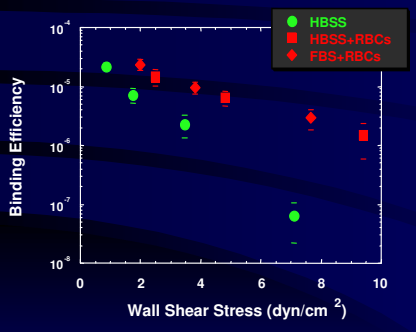

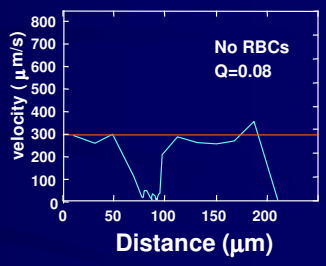

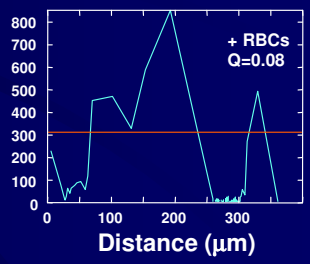

Approaches to the description of a fluid

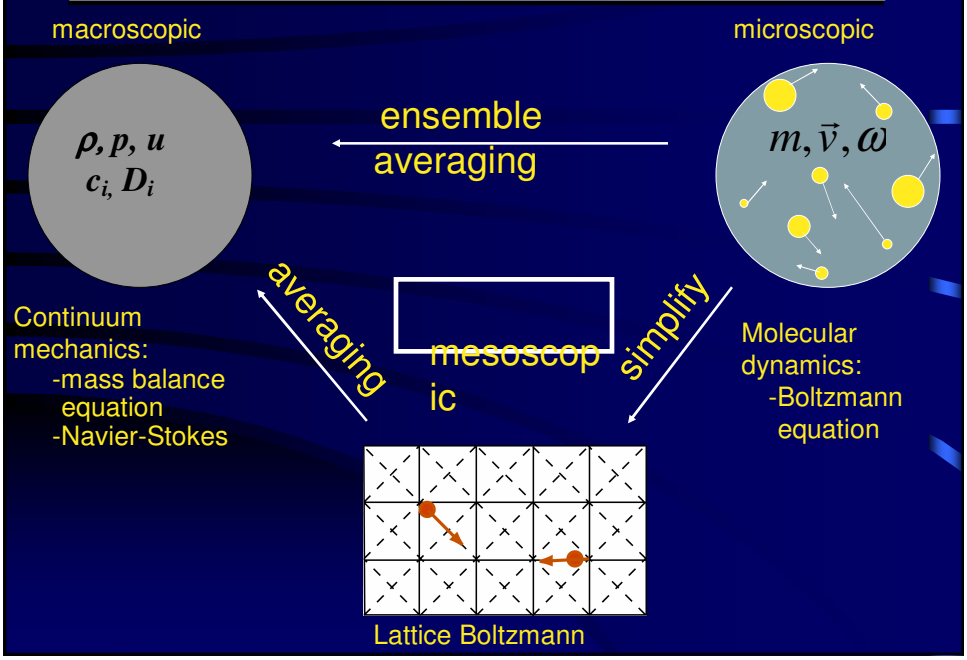

Advantages of the Lattice-Boltzmann approach

- Ø accommodates complex geometries
- Ø adaptable to two-phase flow
- Ø applicable to particle suspensions
- Ø can include diffusion, reaction, precipitation & phase transitions
- Ø handles moving boundaries (e.g. cell deformation, vessel elasticity)
- Ø easily parallelized and scaled-up

Modeling complex fluid dynamics: Lattice Boltzmann

QuickTime™ and a
Cinepak decompressor
are needed to see this picture.

Exa, Inc.

The Lattice Boltzmann model

$$F_i(\vec{x}+\vec{c}_i, t+1) = F_i(\vec{x}, t) + \underbrace{\Omega_i(F_i(\vec{x}, t))}_{\text{Collision}}$$
$$\underbrace{\qquad\qquad\qquad\qquad}_{\text{Propagation}}$$

Collision Back

Propagation

Bounce-

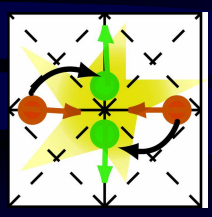

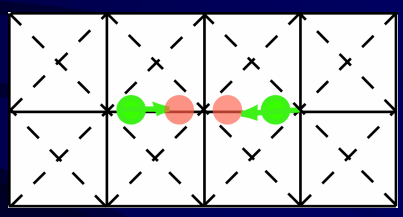

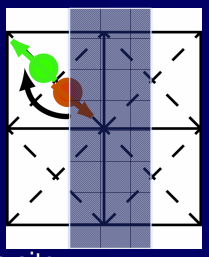

Change in velocity

Mass and momentum are conserved

Packets of fluid move from site to site on the grid at discrete time steps

$t \to t+1$

No-slip boundary conditions

Suspensions of Solid Objects

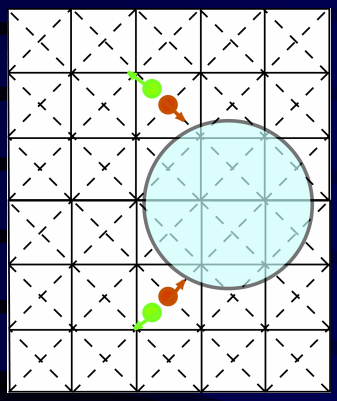

Particle motion follows Newton's law:

$$\frac{d\vec{u}_p}{dt} = \frac{\vec{F}_H}{m_p}$$

$$I \cdot \frac{d\vec{\omega}_p}{dt} + \vec{\omega}_p \times \left[I \cdot \vec{\omega}_p \right] = \vec{T}_H$$

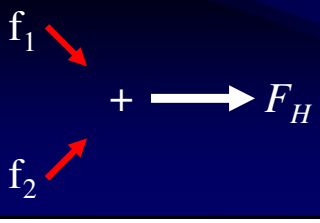

Solution by numerical integration using F

Leukocyte - RBC Dynamics

RBCs (affected by hydrodynamic forces only):

$$\frac{d\vec{u}_{rbc}}{dt} = \frac{\vec{F}_H}{m_{rbc}}$$

Leukocyte dynamics (hydrodynamic forces, ligand forces, colloidal forces):

$$\frac{d\vec{u}_l}{dt} = \frac{\vec{F}_H + \vec{F}_L + \vec{F}_C}{m_l}$$

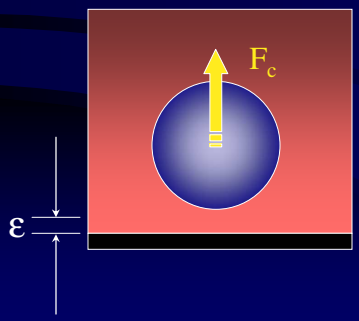

van der Waals-like potential:

$$F_c = \frac{A}{8\sqrt{2}} \sqrt{\frac{R_c}{\varepsilon^5}}$$

Modeling Receptor-Ligand Interactions

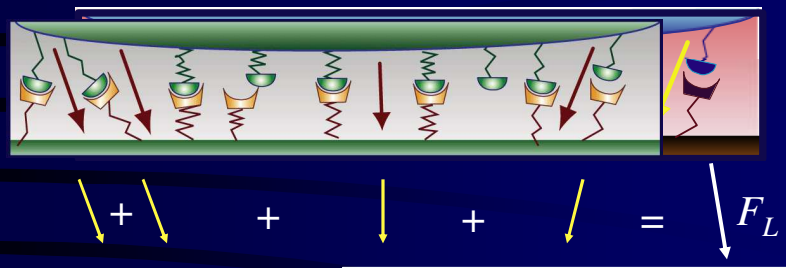

New bond formation $P_f = 1 - \exp(-k_{on}\Delta t) \quad yr < H_c$

Breakage of pre-existing bonds depends on load:

$$P_r = 1 - \exp(-k_r \Delta t)$$

$$k_r = k_r^0 \exp\left(\frac{(L-\lambda)^2}{const^2}\right)$$

Force on an individual bond $f = \sigma(L - \lambda)$

Lattice-Boltzmann modeling of RBC-WBC interactions

Particle Flow dynam
Lattice-Boltzmann

Receptor-Ligand bo
Stochastic model

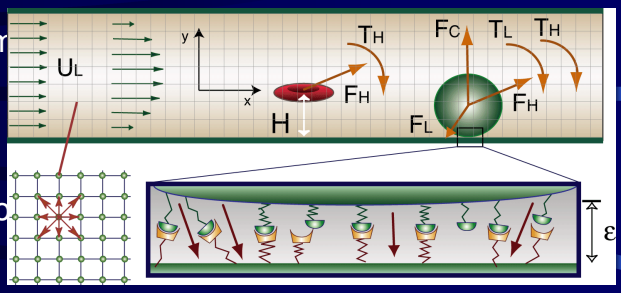

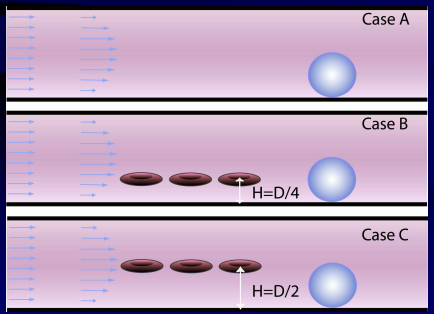

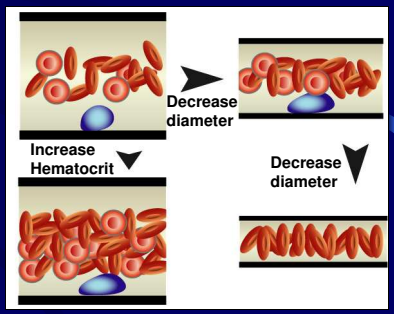

Case A: rolling WBC

D=20μm; Re=0.08; Wall shear rate=150s^{-1}

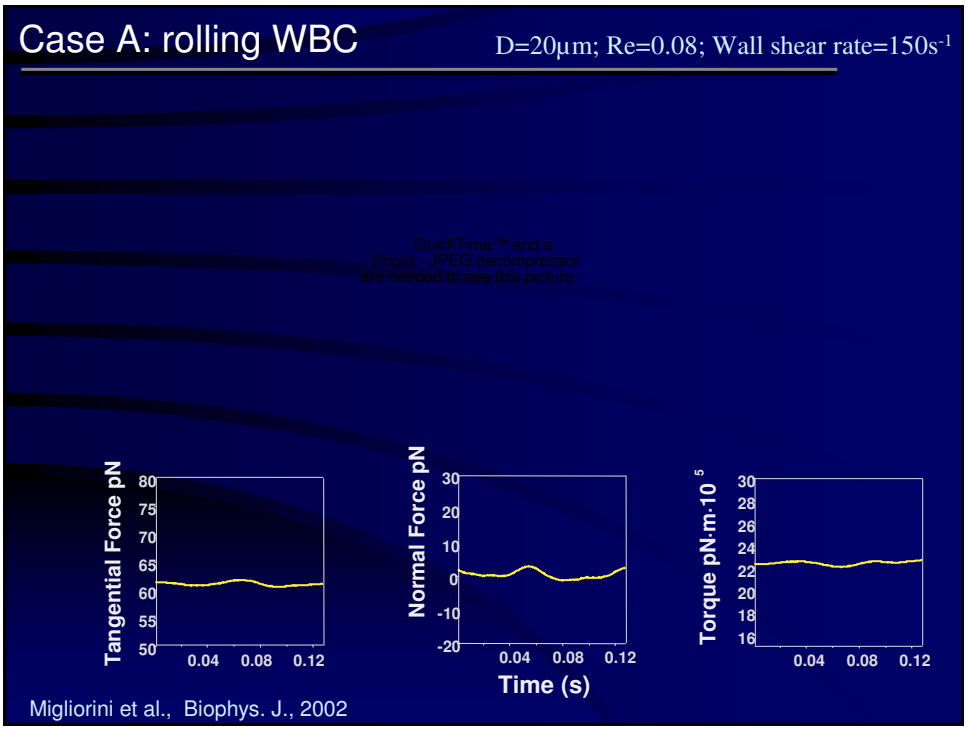

Migliorini et al., Biophys. J., 2002

Case B: head-on collision

D=20μm; Re=0.08; Wall shear rate=150s^{-1}

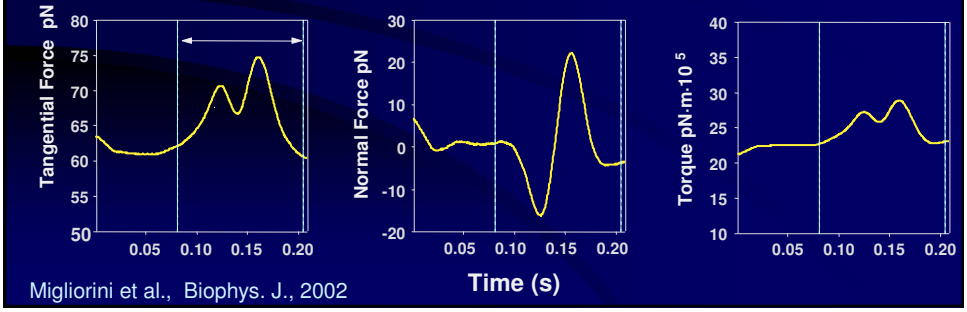

Migliorini et al., Biophys. J., 2002

RBC affects the normal force

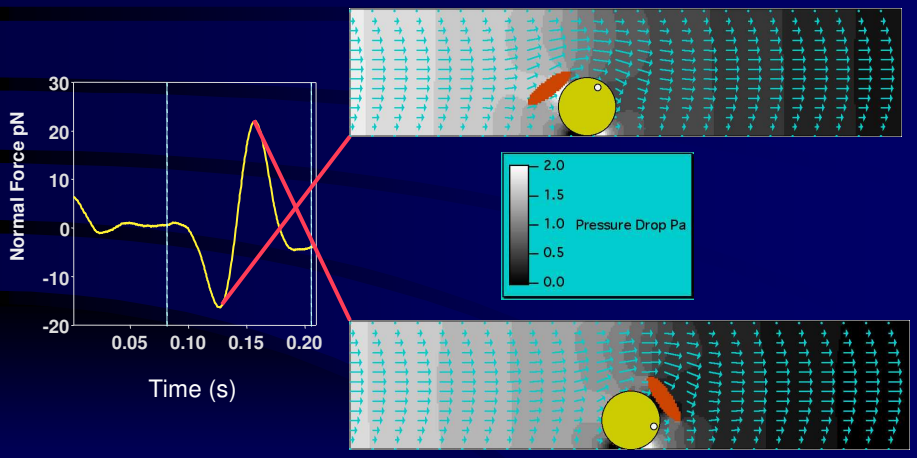

Migliorini et al., Biophys. J., 2002

Case C: glancing collision - Height is critical

QuickTime™ and a
Photo - JPEG decompressor
are needed to see this picture.

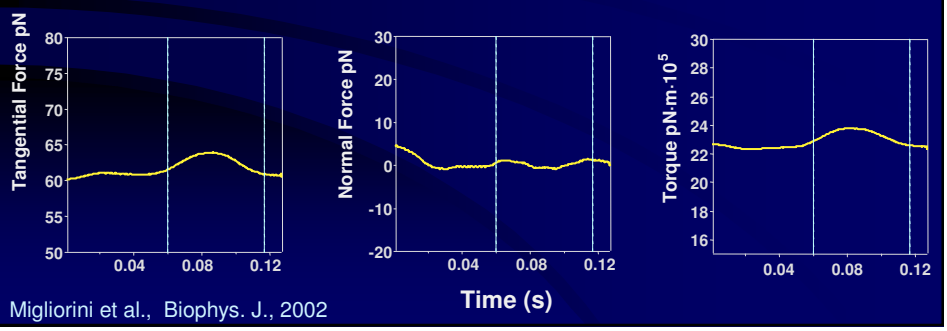

Migliorini et al., Biophys. J., 2002

Significance: Effect of the Hematocrit

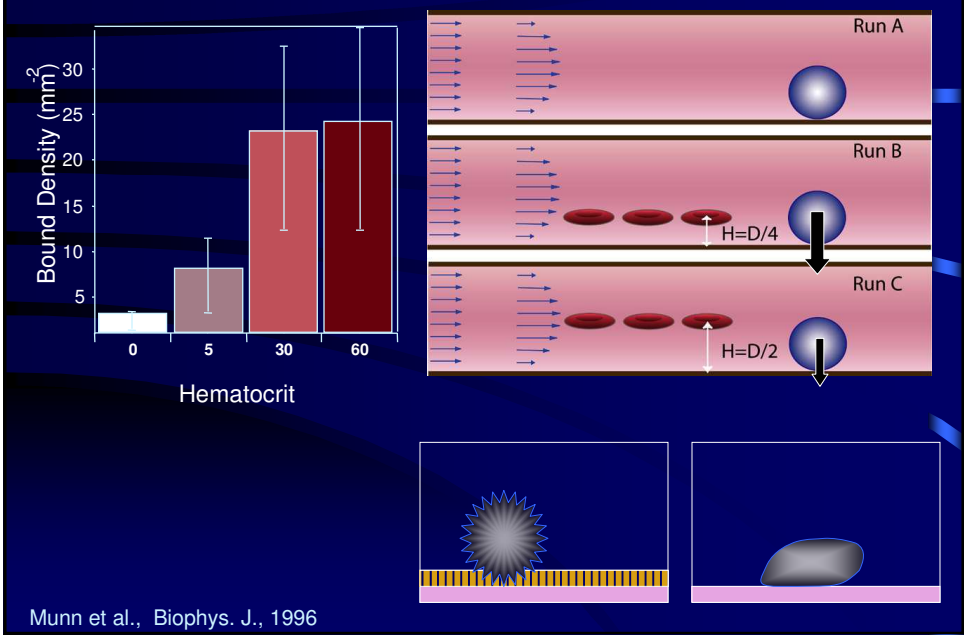

Munn et al., Biophys. J., 1996

Significance: Tangential Force and Torque

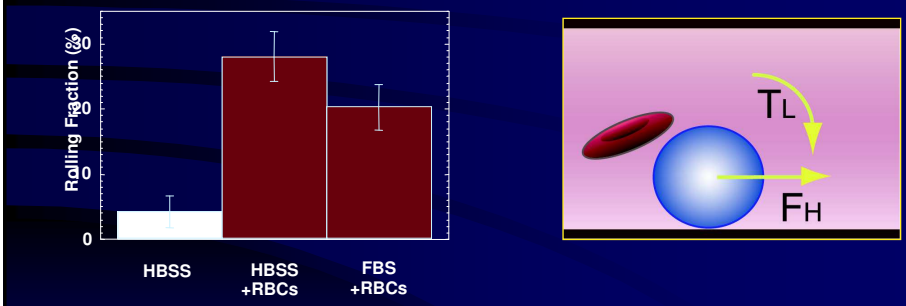

Melder et al., Biophys. J.1995

No RBCs

10.2➡23µm expansion
WSR=588 ➡118s^{-1}
Elapsed time: 0.672s

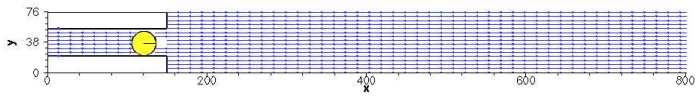

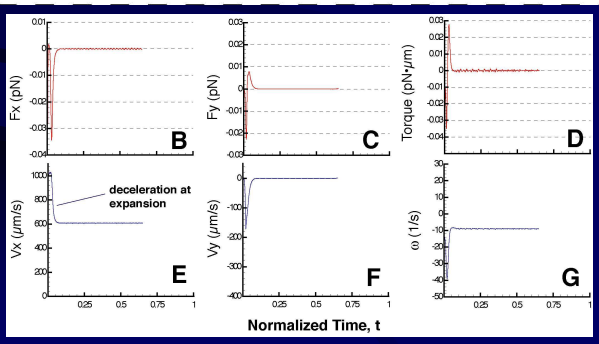

RBCs stack behind WBCs in capillaries

10.2µm capillary
WSR=588s^{-1}
Elapsed time: 1.624s

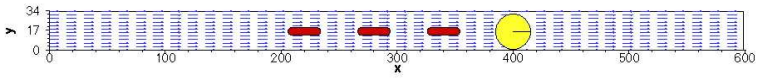

3 RBCs, small expansion

10.2➡23μm expansion
WSR=588 ➡118s^{-1}
Elapsed time: 1.12s

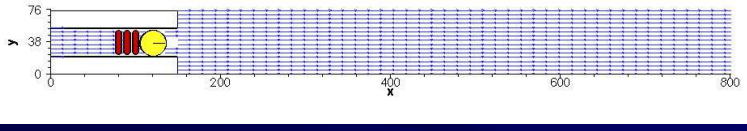

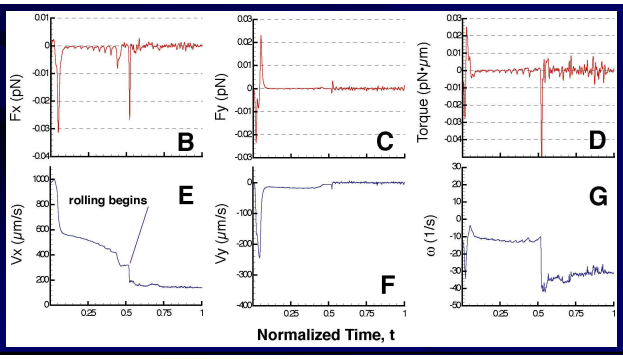

3 RBCs, larger expansion

10.2➡25μm expansion
WSR=588 ➡101s^{-1}
Elapsed time: 1.0s

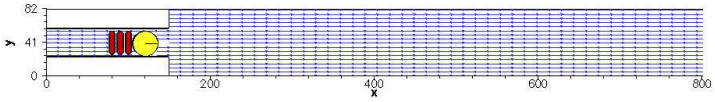

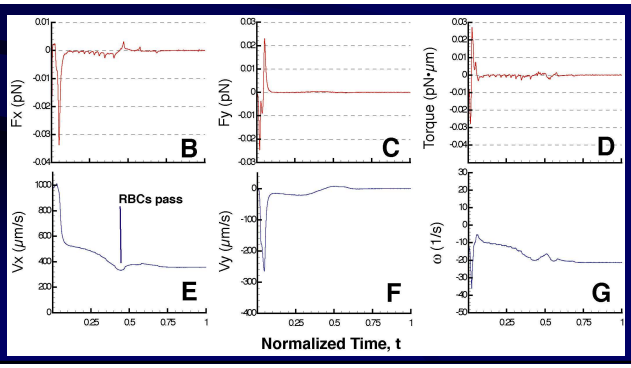

4 RBCs, same expansion

10.2➡25μm expansion
WSR=588 ➡101s^{-1}
Elapsed time: 1.0s

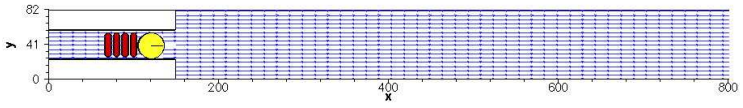

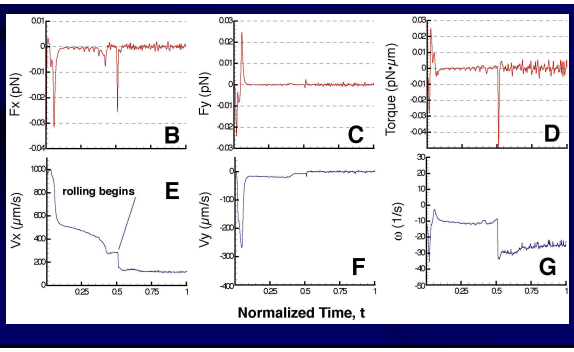

5 RBCs, same expansion

10.2➡25μm expansion
WSR=588 ➡101s^{-1}
Elapsed time: 1.0s

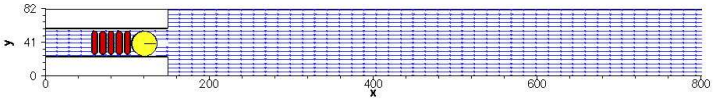

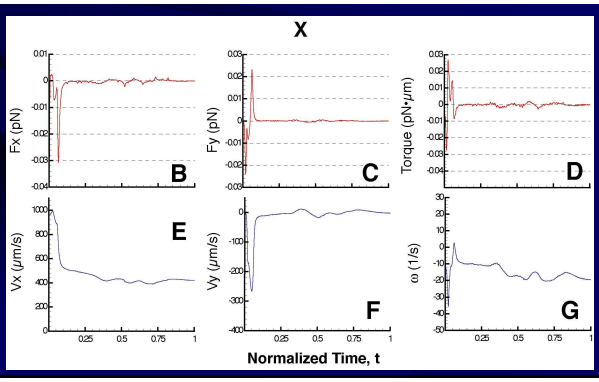

5 RBCs, even larger expansion

10.2➡26μm expansion
WSR=588 ➡88s^{-1}
Elapsed time: 1.064s

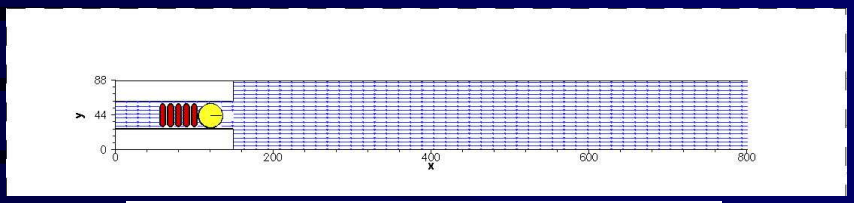

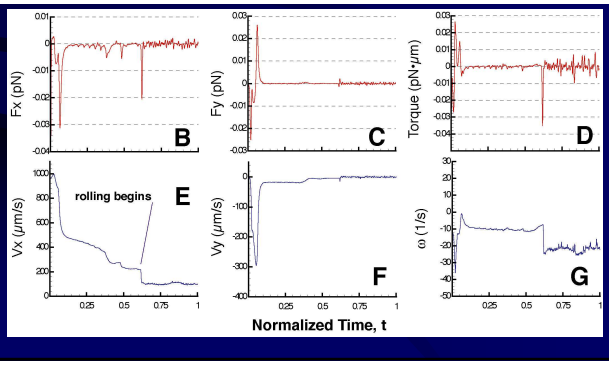

3D reconstruction of normal vasculature

QuickTime™ and a
Video decompressor
are needed to see this picture.

Brown et al. Nature Medicine (2001)

3D reconstruction of tumor vasculature

QuickTime™ and a decompressor are needed to see this picture.

Brown et al. Nature Medicine (2001)

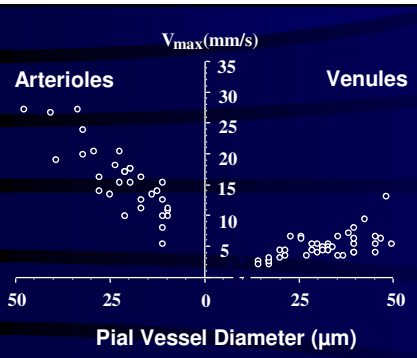

Tumor vessel shear stress levels differ from normal vessels

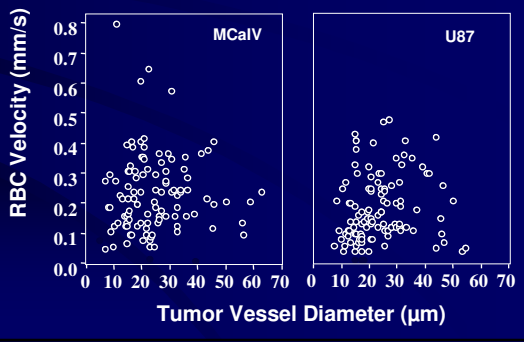

Yuan et al., Cancer Research,

Conclusions

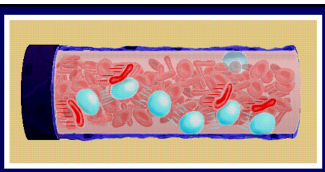

- Model allows estimation of the normal & tangential forces and torque on leukocytes rolling in physiologic flow fields and geometries
- Normal force fluctuations due to RBC collisions can enhance leukocyte adhesion
- Tangential force and torque due to RBCs can encourage leukocyte rolling
- All forces are sensitive to the orientation of collision (and therefore hematocrit and geometry)
- Initiation of rolling at postcapillary venules depends on

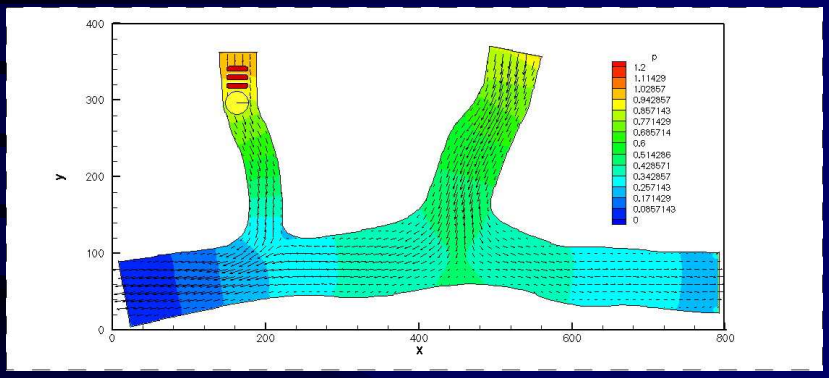

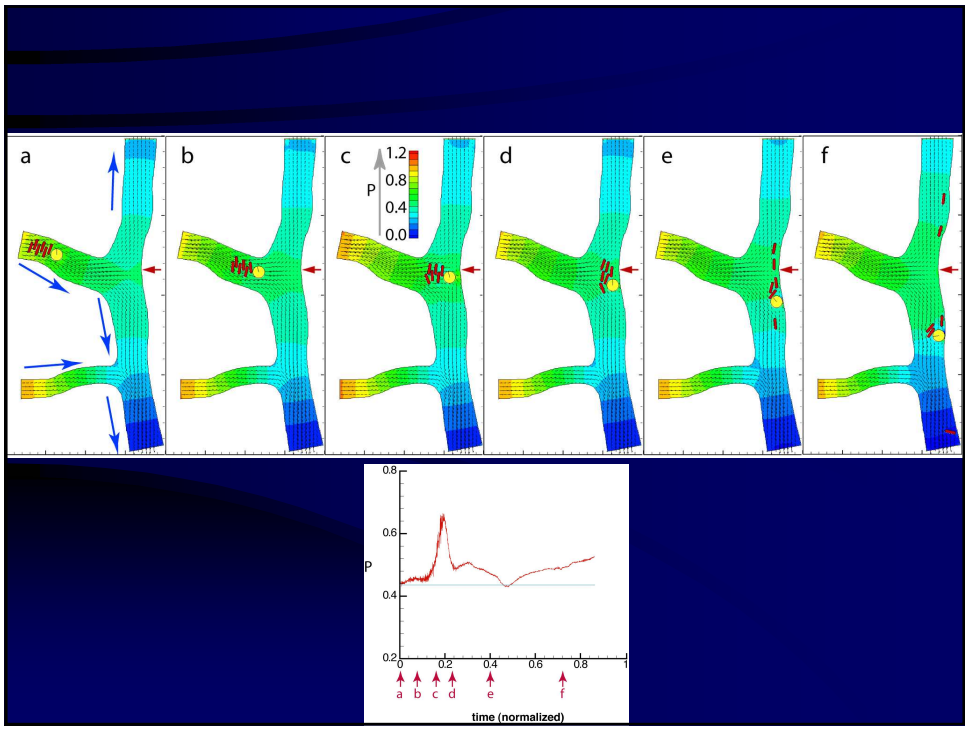
a
b
c
d
e
f
P
1.2
0.8
0.4
0.0
0.8
0.6
0.4
0.2
0
0.2
0.4
0.6
0.8
a b c d e f
time (normalized)

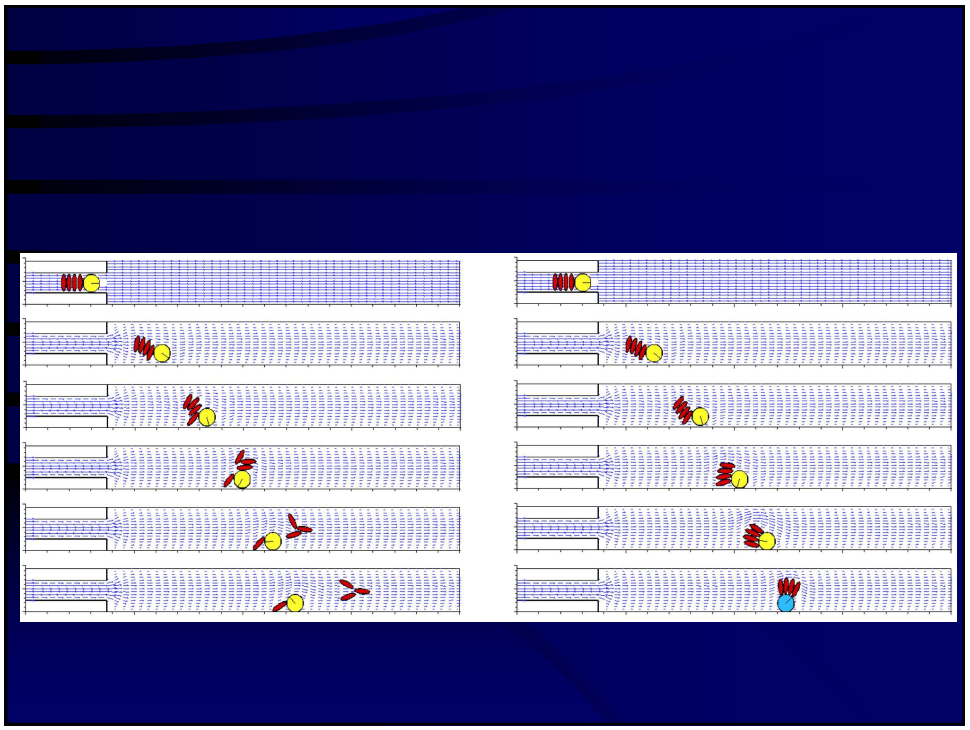

Acknowledgments

Chris Willett

Saroja Ramanujan

Brian Stoll

Cristiano Migliorini

Chenghai Sun

Rakesh Jain

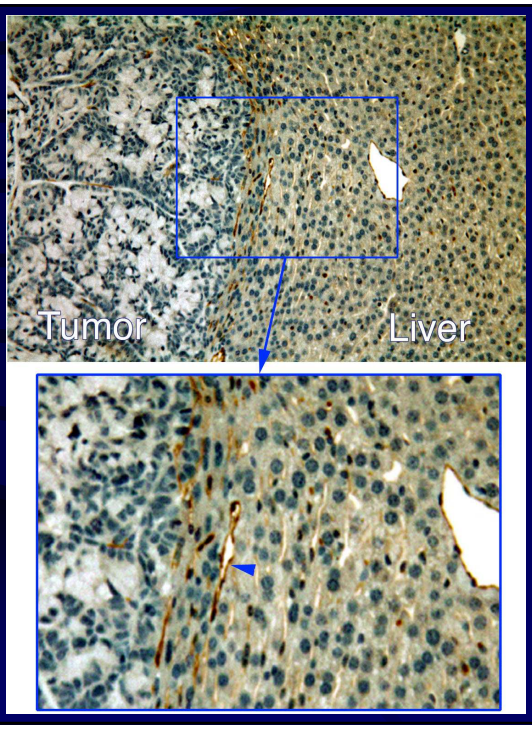

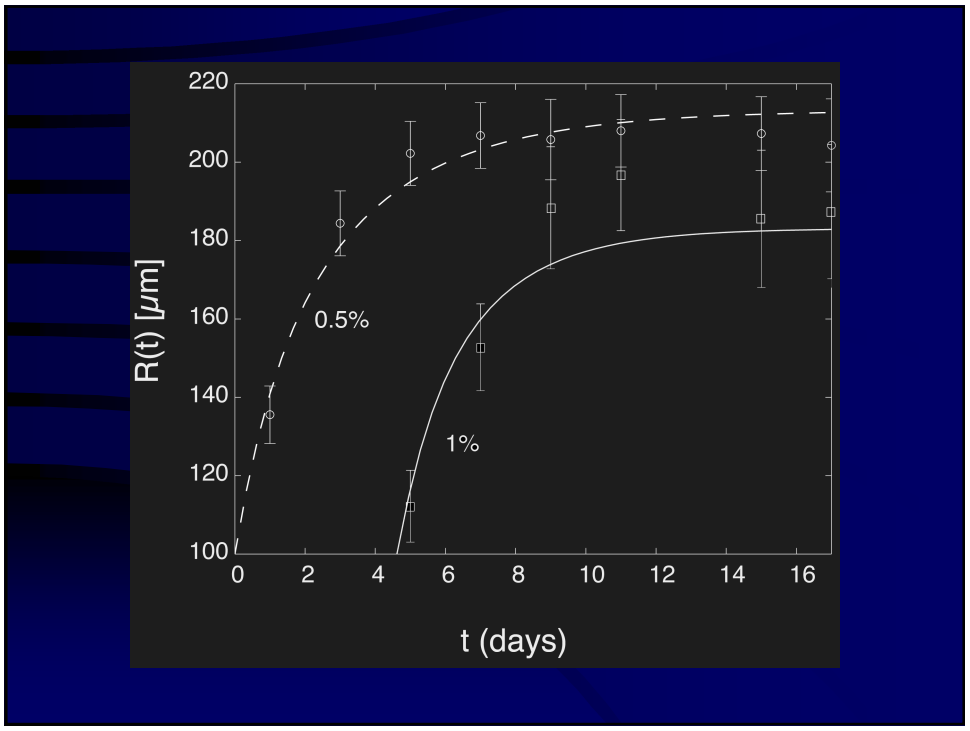
R(t) [μm]
t (days)
0.5%
1%

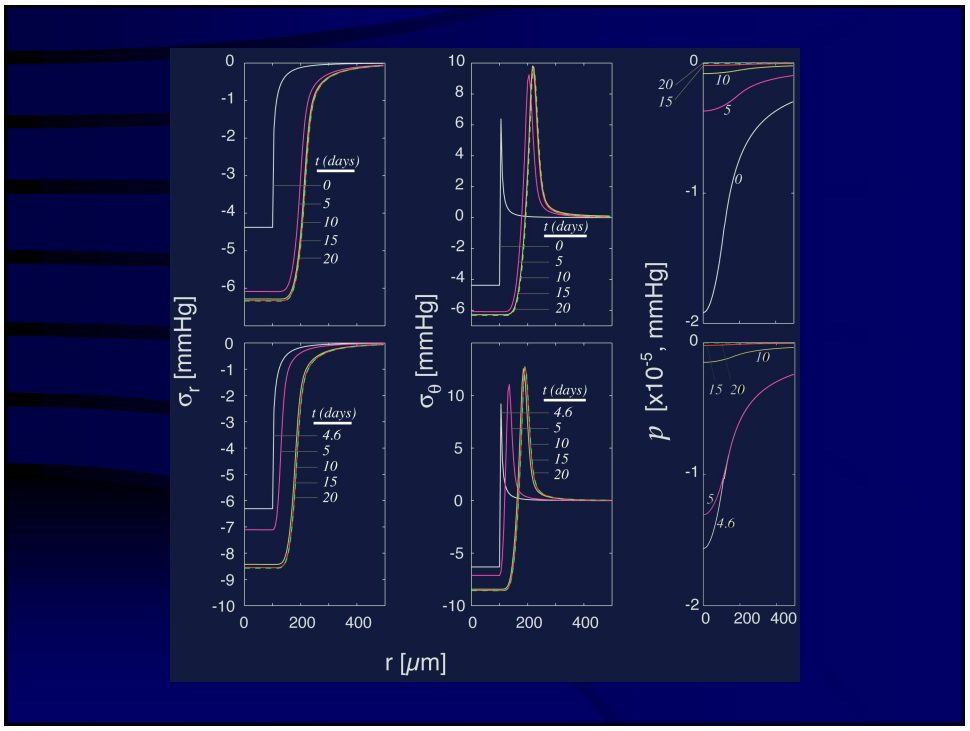
σr [mmHg]
σθ [mmHg]
p [x10-5, mmHg]
r [μm]
t (days)
0
5
10
15
20
4.6

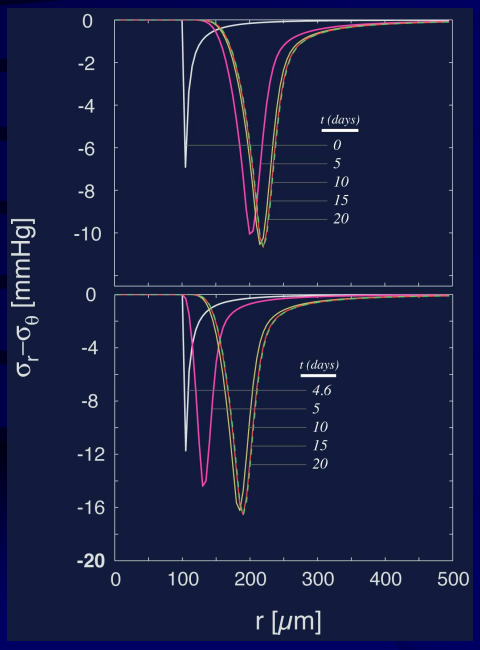
0
-2
-4
-6
-8
-10
t (days)
0
5
10
15
20
0
-4
-8
-12
-16
-20
t (days)
4.6
5
10
15
20
$\sigma_r - \sigma_\theta$ [mmHg]
0
100
200
300
400
500
r [μm]

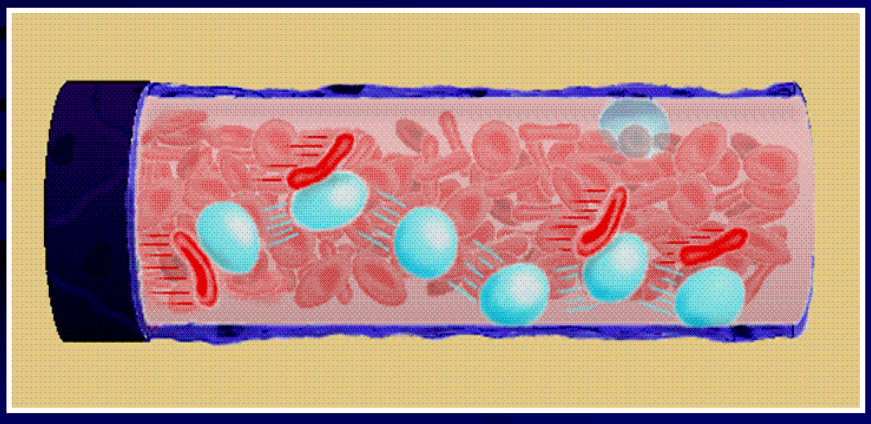

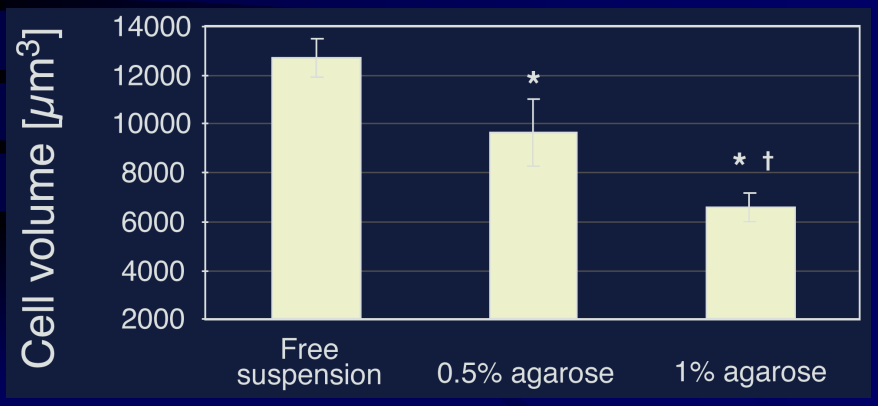

Integrative Pathophysiology:

Mathematical modeling in Cancer

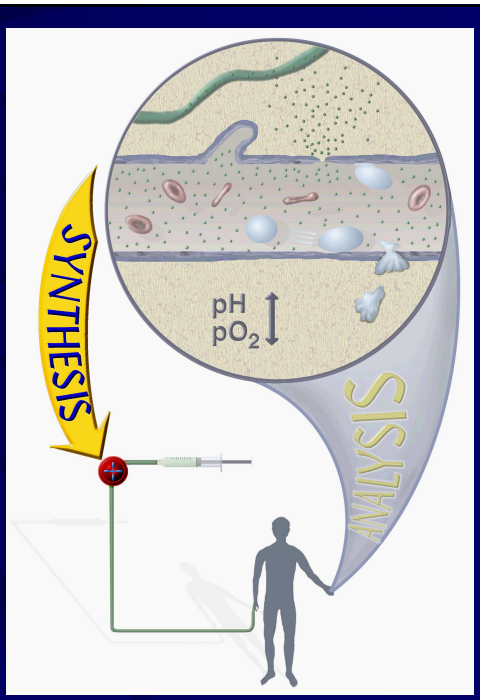

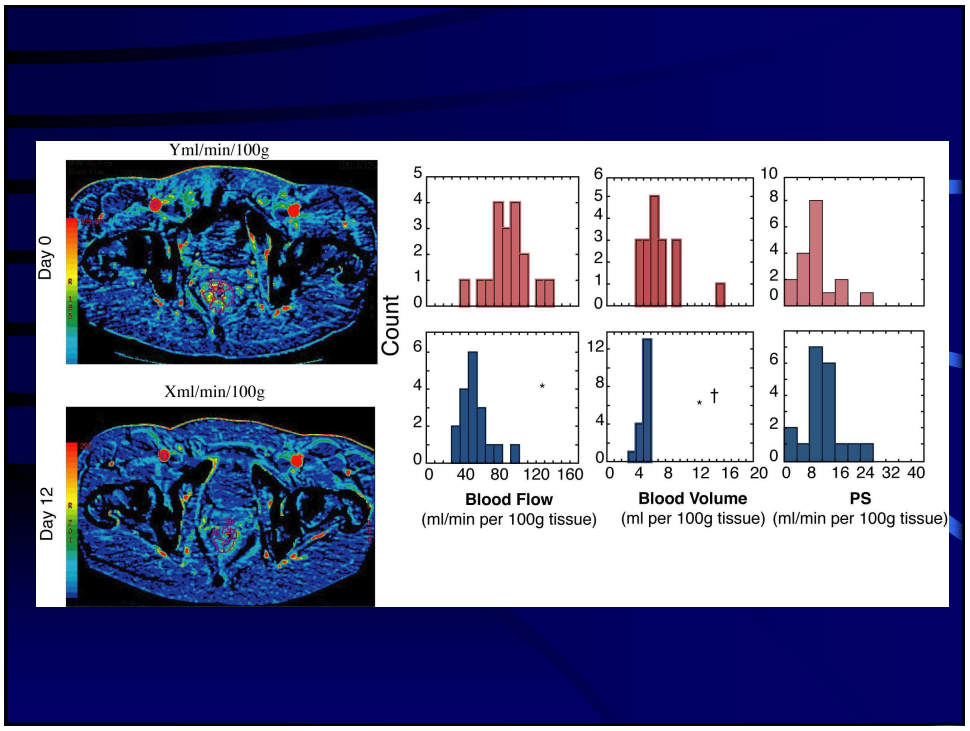
Yml/min/100g
Day 0
Xml/min/100g
Day 12
Count
Blood Flow
(ml/min per 100g tissue)
Blood Volume
(ml per 100g tissue)
PS
(ml/min per 100g tissue)

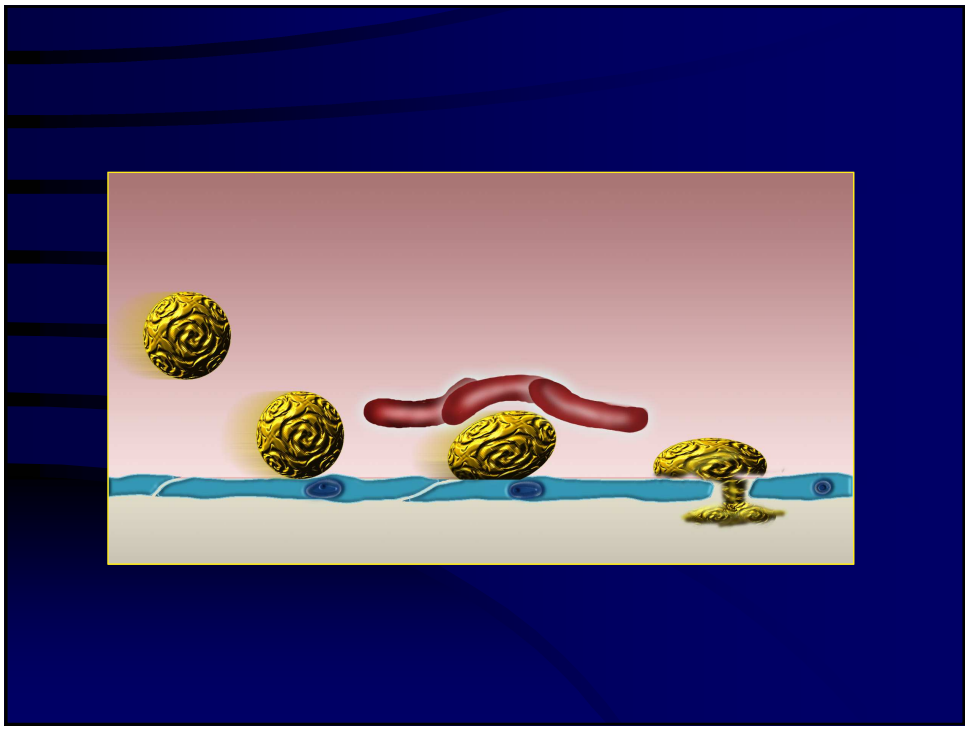

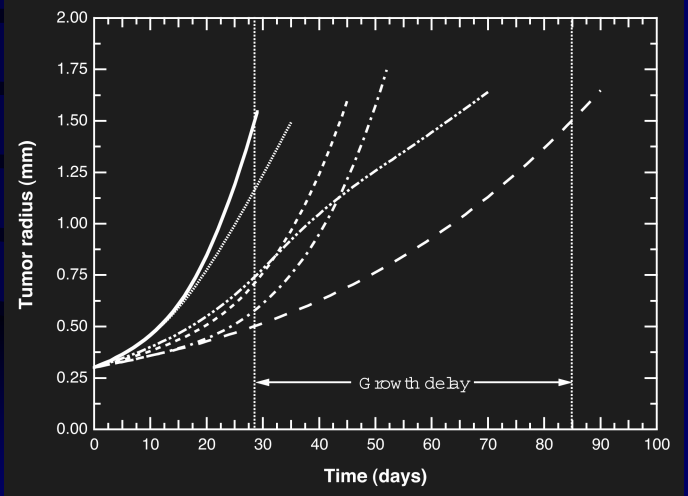

3D reconstruction of normal vasculature

QuickTime™ and a
Video decompressor
are needed to see this picture.

Brown et al. Nature Medicine (2001)

3D reconstruction of tumor vasculature

QuickTime™ and a decompressor are needed to see this picture.

Brown et al. Nature Medicine (2001)